Journal of Materials Chemistry B c8tb00232k

We have presented the Graphical Abstract text and image for your article below. This brief summary of your work will appear in the contents pages of the issue in which your article appears.

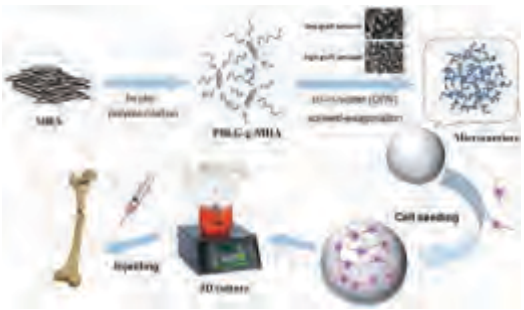

***In situ* polymerization of poly(γ-benzyl-L-glutamate) on mesoporous hydroxyapatite with high graft amounts for the direct fabrication of biodegradable cell microcarriers and their osteogenic induction**

Linlong Li, Xincui Shi, Zongliang Wang,* Yu Wang, Zixue Jiao and Peibiao Zhang*

Through this method, PBLG-*g*-MHA microcarriers with particular properties could be prepared without any non-essential components, such as PLGA.

Please check this proof carefully. **Our staff will not read it in detail after you have returned it.**

Proof corrections must be returned as a single set of corrections, approved by all co-authors. No further corrections can be made after you have submitted your proof corrections as we will publish your article online as soon as possible after they are received.

Please ensure that:

- The spelling and format of all author names and affiliations are checked carefully. Names will be indexed and cited as shown on the proof, so these must be correct.
- Any funding bodies have been acknowledged appropriately.
- All of the editor's queries are answered.
- Any necessary attachments, such as updated images or ESI files, are provided.

Translation errors between word-processor files and typesetting systems can occur so the whole proof needs to be read. Please pay particular attention to: tables; equations; numerical data; figures and graphics; and references.

Please send your corrections preferably as a copy of the proof PDF with electronic notes attached or alternatively as a list of corrections – do not change the text within the PDF file or send a revised manuscript. Corrections at this stage should be minor and not involve extensive changes.

Please return your **final** corrections, where possible within **48 hours** of receipt, by e-mail to: materialsB@rsc.org. If you require more time, please notify us by email.

Funder information

Providing accurate funding information will enable us to help you comply with your funders' reporting mandates. Clear acknowledgement of funder support is an important consideration in funding evaluation and can increase your chances of securing funding in the future. We work closely with Crossref to make your research discoverable through the Funding Data search tool (http://search.crossref.org/funding).

Further information on how to acknowledge your funders can be found on our webpage (http://rsc.li/funding-info).

What is Funding Data?

Funding Data (http://www.crossref.org/fundingdata/) provides a reliable way to track the impact of the work that funders support. We collect funding information from our authors and match this information to funders listed in the Crossref Funder Registry. Once an article has been matched to its funders, it is discoverable through Crossref's search interface.

PubMed Central

Accurate funder information will also help us identify articles that are mandated to be deposited in PubMed Central (PMC) and deposit these on your behalf.

Providing funder information

We have combined the information you gave us on submission with the information in your acknowledgements. This will help ensure funding information is as complete as possible and matches funders listed in the Crossref Funder Registry. **Please check that the funder names and grant numbers in the table are correct.** This table will not be included in your final PDF but we will share the data with Crossref so that your article can be found *via* the Funding Data search tool.

Funder name	Funder ID (for RSC use only)	Award/grant/contract number
National Natural Science Foundation of China	501100001809	51403197, 51473164, 51673186
Chinese Academy of Sciences	501100002367	GJHZ1519, 2017SYHZ0021
Japan Society for the Promotion of Science	501100001691	GJHZ1519
People's Government of Jilin Province	501100003807	2017SYHZ0021

Q1

If a funding organisation you included in your acknowledgements or on submission of your article is not currently listed in the registry it will not appear in the table above. We can only deposit data if funders are already listed in the Crossref Funder Registry, but we will pass all funding information on to Crossref so that additional funders can be included in future.

Researcher information

If any authors have ORCID or ResearcherID details that are not listed below, please provide these with your proof corrections. Please check that the ORCID and ResearcherID details listed below have been assigned to the correct author. Authors should have their own unique ORCID iD and should not use another researcher's, as errors will delay publication.

Please also update your account on our online manuscript submission system to add your ORCID details, which will then be automatically included in all future submissions. See here for step-by-step instructions and more information on author identifiers.

First (given) name(s)	Last (family) name(s)	ResearcherID	ORCID
Linlong	Li		
Xincui	Shi		
Zongliang	Wang		
Yu	Wang		

Zixue	Jiao		
Peibiao	Zhang		0000-0003-0073-6467

Queries for the attention of the authors

Journal: **Journal of Materials Chemistry B**

Paper: **c8tb00232k**

Title: ***In situ* polymerization of poly(γ-benzyl-L-glutamate) on mesoporous hydroxyapatite with high graft amounts for the direct fabrication of biodegradable cell microcarriers and their osteogenic induction**

For your information: You can cite this article before you receive notification of the page numbers by using the following format: (authors), J. Mater. Chem. B, (year), DOI: 10.1039/c8tb00232k.

Editor's queries are marked on your proof like this Q1, Q2, etc. and for your convenience line numbers are indicated like this 5, 10, 15, ...

Please ensure that all queries are answered when returning your proof corrections so that publication of your article is not delayed.

Query reference	Query	Remarks
Q1	Funder details have been incorporated in the funder table using information provided in the article text. Please check that the funder information in the table is correct.	
Q2	Please confirm that the spelling and format of all author names is correct. Names will be indexed and cited as shown on the proof, so these must be correct. No late corrections can be made.	
Q3	The article title has been altered for clarity. Please check that the meaning is correct.	
Q4	In the sentence beginning ''Traditional plane cell culture methods...'', the meaning of the word ''plane'' is unclear, please check if it should be ''plain''.	
Q5	Please check that the footnotes have been displayed correctly in Table 1.	
Q6	The meaning of the word ''Material'' in the sentence beginning ''Material thin film...'' is not clear – please provide alternative text.	
Q7	The sentence beginning ''As shown in Fig. S2(c)...'' has been altered for clarity, please check the meaning has not changed.	
Q8	The phrase ''before 5 days'' in the sentence beginning ''Additionally, the pH value of...'' is unclear, please confirm if this should be changed to ''after 5 days''.	
Q9	Ref. 22: Can this reference be updated? If so, please provide the relevant information such as year, volume and page or article numbers as appropriate.	

Journal of Materials Chemistry B

PAPER

In situ polymerization of poly(γ-benzyl-L-glutamate) on mesoporous hydroxyapatite with high graft amounts for the direct fabrication of biodegradable cell microcarriers and their osteogenic induction†

Linlong Li,[ab] Xincui Shi,[a] Zongliang Wang,*[a] Yu Wang,[a] Zixue Jiao[a] and Peibiao Zhang *[ab]

Cite this: DOI: 10.1039/c8tb00232k

Received 25th January 2018,
Accepted 10th April 2018

DOI: 10.1039/c8tb00232k

rsc.li/materials-b

Large-scale cell culture for cell expansion in tissue engineering is currently a major focus of research. One method to achieve better cell amplification is to utilize microcarriers. In this study, different amounts of poly(γ-benzyl-L-glutamate) (PBLG) (from 11 wt% to 50 wt%) were grafted on mesoporous hydroxyapatite (MHA) by the *in situ* ring opening polymerization of γ-benzyl-L-glutamate *N*-carboxyanhydride (BLG-NCA), and biodegradable and biocompatible PBLG-*g*-MHA microcarriers were directly fabricated using the oil-in-water (O/W) solvent-evaporation technique for bone tissue engineering. The amount of grafted PBLG could be controlled by adjusting the feed ratio of MHA and BLG-NCA. The relationships between sphere morphology and graft amount or solution concentration were explored. Furthermore, cytological assays were performed to evaluate the biological properties of the PBLG-*g*-MHA microcarriers. For a solution concentration of 3% (w/v) and PBLG graft amounts of 33 wt% and 50 wt%, the microspheres could be harvested with optimal spherical shapes. *In vitro* cell culture revealed that the PBLG-*g*-MHA microspheres had favorable properties for cell proliferation and significantly enhanced the osteogenic differentiation of MC3T3-E1 cells and bone matrix formation.

1. Introduction

Large-scale cell culture has become a focus of research for the production of biochemicals (such as interferons, enzymes, and antibodies)[1] and cell expansion in tissue engineering.[2,3] Traditional plane cell culture methods are not suited for cell expansion at a large scale because the space for growth is not sufficient and the nutrient supply is poor as the culture time increases. One way to achieve better large-scale cell culture is to utilize microcarriers.[1,4] Microcarriers are spheres that can act as the support matrix for the growth of anchorage-dependent cells in bioreactors and they were firstly reported by van Wezel in 1967.[5] Owing to the large specific area of microcarriers, which enables the sufficient exchange of nutrients and metabolic waste with the culture medium, they are quite efficient for cell amplification in tissue engineering.[6] Additionally, microcarriers have a 3-D spatial structure similar to the environment of cells *in vivo* and they are beneficial for cell migration and proliferation.[7] The ability of cell attachment to the microcarrier surface depends on the chemical composition, surface topography and porosity of microcarriers.[8] Therefore, the design and fabrication of microcarriers play an important role in the biomedical applications.[9]

Many efforts have been made to fabricate appropriate microcarriers for different cell types. Various materials, such as polystyrene,[10] dextran,[11] and silica glass beads,[12] have been used to prepare microcarriers. When used *in vivo*, biodegradable matrixes are especially useful, because traditional cell microcarriers, such as Sephadex beads (Cytodex-3) and Cultispher series, are nondegradable.[13] Cells cultured on nondegradable microcarriers usually have to be harvested by enzymatic digestion or mechanical dissociation because they cannot be used directly in the body. And cell activity might be affected by the digestion or the dissociation process. In contrast, biodegradable materials could be absorbed in the body. Thus, biodegradable microcarriers after cell seeding can be used directly.[14] Some synthetic biodegradable polymers, such

[a] *Key Laboratory of Polymer Ecomaterials, Changchun Institute of Applied Chemistry, Chinese Academy of Sciences, 5625 Renmin Street, Changchun 130022, P. R. China. E-mail: wangzl@ciac.ac.cn, zhangpb@ciac.ac.cn; Fax: +86-431-85262058; Tel: +86-431-85262058*

[b] *University of Chinese Academy of Sciences, 19 Yuquan Road, Beijing 100049, P. R. China*

† Electronic supplementary information (ESI) available. See DOI: 10.1039/c8tb00232k

as poly(lactic acid) (PLA), poly(glycolic acid) (PGA), and their copolymer poly(lactic acid–glycolic acid) (PLGA), have attracted increasing attention owing to their biodegradability and biocompatibility. They are widely used in various biomedical applications, such as drug delivery,[15] tissue engineering,[16,17] and microcarriers for cell culture or therapy.[18] Newman *et al.* reported that PLGA microspheres encapsulated with retinoic acid induce P19 cell differentiation into neurons, demonstrating the potential application of these microspheres as transplantation matrices for pluripotent stem cells in tissue engineering and regeneration.[18] In another study, Savi *et al.*[19] reported the delivery of human adipose-derived stem cells (ADSCs) by PLGA microcarriers loaded with hepatocyte growth factor (HGF) and insulin-like growth factor-1 (IGF-1) for the treatment of myocardial infarction and observed a marked increase of ADSC engraftment 2 weeks after injection as well as the stimulation of healing in the chronically infarcted myocardium. Therefore, biodegradable microcarriers have excellent properties for the direct delivery of both drugs and stem cells, with a wide range of applications in the field of tissue engineering.

Composites of biodegradable polymers containing hydroxyapatite (HA) are widely used in the field of bone tissue engineering because they closely mimic natural bone and have excellent biocompatibility and bone integration ability.[20–22] Pure HA ceramics are brittle and the lack of processability limits their clinical applications.[23] The combined utilization of polymer biomaterials may overcome this limitation. As a component, nano-HA can neutralize the acidic degradation products of biodegradable polymers and thus maintain suitable conditions for cell growth.[24] The surface roughness of the nanocomposite could enhance the attachment, proliferation, and differentiation of bone-forming cells.[21,25] In our previous study, biodegradable microcarriers of PLGA/HA immobilized with insulin-like growth factor 1 (IGF-1) *via* polydopamine were prepared and the synergetic effects of HA and IGF-1 on the differentiation of mouse ADSCs were achieved.[14] These results showed that HA/PLGA microcarriers could be used as injectable biomaterials for bone tissue engineering and HA played an important role in accelerating or inducing the attachment, proliferation, and differentiation of osteogenic cells.

Although PLGA is biodegradable and biocompatible, it is a hydrophobic polymer and lacks cell binding sites. Poly(α-amino acids) and their derivatives are a series of natural or synthetic biodegradable polymers. Their degradation products are short peptides or α-amino acids with better biocompatibility compared to that of PLA or PLGA. Among all the amino acids, glutamate seems to be associated with bone cell signaling and intercellular communication.[26] PBLG is one of the earliest synthesized and most widely studied poly(α-amino acids) for controlled drug release[27] and gene delivery.[28,29] Furthermore, Ravichandran *et al.*[30] fabricated PLA/PBLG/collagen scaffolds using the electrospinning method with HA deposition. ADSCs can undergo osteogenic differentiation on these scaffolds owing to the calcium binding moiety of PBLG and the osteoconductivity of HA. In our previous work,[31] PBLG was grafted onto HA to improve the interfacial compatibility between HA and the polymer matrix, and PBLG-*g*-HA showed enhanced biocompatibility, adhesion, and proliferation of osteoblasts. Liao *et al.*[32] fabricated PBLG-modified hydroxyapatite/poly(L-lactic acid) (PBLG-*g*-HA/PLLA) composites and demonstrated that the PBLG-*g*-HA/PLLA composite materials induce high levels of new bone formation *in vivo*.

In the present study, mesoporous HA (MHA) with different graft amounts of PBLG (PBLG-*g*-MHA) was synthesized and employed to directly fabricate biodegradable and biocompatible microcarriers for bone tissue engineering. Graft amounts were controlled from 11.82 wt% to 50.30 wt% by varying the feeding ratio. Microcarriers were fabricated by the oil-in-water (O/W) solvent-evaporation technique. The relationships between sphere morphology and graft amount or solution concentration were explored. Furthermore, biological experiments were performed to compare the specific biological properties of PBLG-*g*-MHA and the MHA/PLGA microcarriers.

2. Experimental

2.1 Materials

Calcium chloride ($CaCl_2$), diammonium hydrogen phosphate [$(NH_4)_2HPO_4$], and sodium hydroxide (NaOH) were purchased from Beijing Chemical Works (Beijing, China). 3-Aminopropyltriethoxysilane (APS) was purchased from Tokyo Chemical Industry (Tokyo, Japan). γ-Benzyl-L-glutamate acid was purchased from Sinopharm Chemical Reagent Co., Ltd (Shanghai, China). Ethanol, tetrahydrofuran (THF), dioxane, and acetone were purchased from Beijing Chemical Works. *N*-Methylpyrrolidone (NMP) was purchased from Aladdin Biochemical Technology Co., Ltd (Shanghai, China).

2.2 Synthesis of MHA and APS-modified MHA

MHA was synthesized according to our previous study[33] and APS-modified MHA (MHA-APS) was synthesized based on published methods.[31] Briefly, 3.17 g of $(NH_4)_2HPO_4$ and 8.74 g of cetyltrimethyl-ammonium bromide (CTAB) were dissolved in 100 mL of deionized water and the solution was adjusted to pH 12 using a NaOH solution. Subsequently, 4.44 g of $CaCl_2$ was dissolved in 60 mL of deionized water. The $CaCl_2$ solution was added dropwise to the $(NH_4)_2HPO_4$ and CTAB solution mixture, and the system was refluxed at 120 °C for 24 h. The precipitate was washed several times with ethanol and then deionized water. After drying at 70 °C for 48 h, the product was then calcined in a box furnace (Thermo Fisher, Waltham, MA, USA) at 550 °C for 6 h to remove the template CTAB. Subsequently, 0.44 g of APS was added to the alcohol solution, which contained 180 mL of alcohol and 20 mL of deionized water. The solution was stirred for 0.5 h and 2 g of MHA was then added. The mixture was subjected to ultrasonic treatment for 15 min and then stirred for another 6 h at 25 °C. The product was centrifuged and washed with ethanol three times. Subsequently, the powder was dried at room temperature and cured

at 130 °C for 2 h in a drying oven to strengthen the polysiloxane network structure.

2.3 Synthesis of BLG-NCA

γ-Benzyl-L-glutamate *N*-carboxyanhydride (BLG-NCA) was synthesized according to previously reported methods.[34] Briefly, 20 g of BLG (0.0843 mol) and 14 g of triphosgene (0.0472 mol) were added to 180 mL of dried THF and the solution was heated to 55 °C under a nitrogen atmosphere. The reaction system was stirred for approximately 40 min at 55 °C until the solution became transparent; the mixture was then poured slowly into 1200 mL of petroleum ether and a white precipitate appeared immediately. The white product was filtered and recrystallized 3 times from anhydrous ethyl acetate and petroleum ether (3 : 1, volume ratio), successively. Then, the white precipitate was filtered and vacuum dried to obtain the product BLG-NCA (yield: 71.3%).

2.4 Synthesis of PBLG-*g*-MHA

APS-MHA (0.5 g) and various amounts of BLG-NCA (see Table 1) were added to a flame-dried 100 mL round-bottom flask, and the air in the flask was extracted and replaced with water-free high-purity nitrogen. Subsequently, 60 mL of dried dioxane was injected into the flask. The mixture was dispersed by ultrasonic treatment for 15 min and then stirred for 32 h at 25 °C. The resulting materials were collected and washed with dioxane and acetone, respectively. The products were dried at room temperature.

2.5 Preparation of microspheres

PBLG-*g*-MHA microspheres were prepared by the O/W solvent-evaporation technique.[35] Briefly, various concentrations of PBLG-*g*-MHA/$CHCl_3$ solutions (1%, 3%, and 5%, w/v) were prepared by dissolving the corresponding amounts of PBLG-*g*-MHA in trichloromethane to obtain homogeneous systems. The solutions were then poured into 200 mL of deionized water containing 0.15% PVA (w/v) with stirring at 750 rpm using a magnetic stirrer. Agitation was continued for 6 h at 25 °C to achieve complete evaporation of the organic solvent. The produced microspheres were collected by centrifugation, thoroughly washed with deionized water three times, and then dried under reduced pressure. As the control group, MHA/PLGA microspheres were also prepared by the same technique. As previous work reported,[36] the highest grafting amount of PLLA on nano-HA was about 22 wt%. In our work, the graft amount of PBLG could be achieved at a level of about 50%. Thus, PLGA-*g*-HA composite materials with a high graft amount could easily be obtained. Then, the physical blending method was utilized to fabricate the MHA/PLGA microspheres. According to the constitution of PBLG-*g*-MHA with different PBLG grafting amounts, namely the ratio of the organic part to the inorganic part, the corresponding amounts of PLGA and MHA were weighed and then MHA/PLGA/$CHCl_3$ solutions were prepared through the same method as mentioned above.

2.6 Characterization

2.6.1 Material characterization. The X-ray diffraction (XRD) data for the materials from 20° to 70° were obtained using a Bruker D8 Advance X-Ray Diffractometer with a Cu tube anode. Fourier-transform infrared spectroscopy (FT-IR, Bio-Rad Win-IR Spectrometer, Watford, UK) spectra were recorded using the KBr slice method. N_2 adsorption/desorption isotherms were collected in a Quantachrome Autosorb-1 gas adsorption analyzer at 78 K after degassing the samples at 453 K for 24 h. The relative pressure P/P_0 of the isotherm was studied from 0.01 to 1.0. The surface areas of the sample powders were calculated according to the Barrett–Emmett–Teller (BET) equation. The pore parameters were calculated from the desorption branches of the isotherm using the Barrett–Joyner–Halanda model. The amounts of PBLG surface-grafted MHA and HA were characterized by thermal gravimetric analysis (TGA) (TA Instruments TGA500, USA) by heating the samples from 25 °C to 800 °C at a rate of 10 °C min^{-1} in air. The morphology and size distribution of the microspheres were characterized by scanning electron microscopy (XL-30 ESEM FEG Scanning Electron Microscope; FEI Company, Hillsboro, OR, USA) and using an Energy Dispersive X-ray Detector (X-MAX; Oxford Instruments, Abingdon, UK). The samples were observed after gold coating using a sputter-coater. The amount of grafted PBLG (GA%) and the grafting efficiency (GE%) were calculated according to the following formulae:

$$\mathrm{GA}\ (\%) = W_{(\text{PBLG-}g\text{-MHA})} - W_{(\text{MHA-APS})}$$

(where $W_{(\text{PBLG-}g\text{-MHA})}$ represents the weight loss of the PBLG-*g*-MHA sample and $W_{(\text{MHA-APS})}$ is the weight loss of MHA-APS),

$$\mathrm{GE}\ (\%) = M_{(\text{PBLG})}/M_{(\text{NCA})}$$

(where $M_{(\text{PBLG})}$ is the mass of the surface-grafted PBLG calculated by the graft ratio of a certain amount of PBLG-*g*-MHA, and

Table 1 Graft amount and reaction efficiency of MHA-APS and PBLG-*g*-MHA related to reaction conditions analyzed by TGA

Samples	Feed ratio (w/w) MHA-APS : NCA	Reaction time (h)	Graft amount[a] (%)	Graft efficiency[b] (%)
MHA-APS	—	—	1.80	—
PBLG-*g*-MHA-1	1 : 0.25	32	11.82	53.61
PBLG-*g*-MHA-2	1 : 0.5	32	22.38	57.66
PBLG-*g*-MHA-3	1 : 1	32	33.12	49.52
PBLG-*g*-MHA-4	1 : 2	32	50.30	50.60

[a] Graft amount of APS (GA%): GA (%) = $W_{(\text{MHA-APS})} - W_{(\text{MHA})}$ (%). Graft amount of PBLG (GA%): GA (%) = $W_{(\text{PBLG-}g\text{-MHA})} - W_{(\text{MHA-APS})}$ (%). [b] Graft efficiency (GE%): GE (%) = $M_{(\text{PBLG})}/M_{(\text{NCA})}$ (%).

$M_{(NCA)}$ is the mass of BLG-NCA used in the reaction according to the correlative feed ratio (shown in Table 1)).

The wetting properties of PBLG-*g*-MHA were determined based on measurements of the contact angle. Material thin film coatings on coverslips were prepared according to the method as follows. Briefly, siliconized coverslips of 18 mm × 18 mm were prepared by treatment with 2% (v/v) trimethylchlorosilane/$CHCl_3$ solution, followed by baking at 180 °C for 4 h. All the products were dissolved in $CHCl_3$ with a concentration of 3% (w/v). Subsequently, 25 μL of the solution was added dropwise to a coverslip and then another coverslip was coated on the previous one. Then, the two coverslips were separated to form a thin film on each coverslip. The thin films were dried under a vacuum for 24 h at room temperature. The static contact angle measurements were obtained using a Krüss DSA 10 instrument (Germany) following the standard sessile drop method with ultrapure water. At least five droplets were dropped onto the same membrane and their contact angles were analyzed using software provided by the manufacturer.

2.6.2 Biodegradation of microspheres. Each group of microspheres (15 mg) was added to an Eppendorf tube and 5 mL of phosphate-buffered saline (PBS, pH = 7.4) was injected to pre-wet the spheres. After 1 h, another 5 mL of PBS was added to the tubes. The tubes were placed in an incubator at 37 °C and the medium was changed 2 times per week. Microspheres were collected after 1, 2, 3, and 4 weeks, washed with deionized water 3 times, and vacuum-dried for further SEM analysis.

2.6.3 Cell culture, viability, and morphology. To investigate the different effects of PBLG-*g*-MHA on cell viability in 2-D and 3-D cultures, thin films on cover glasses were prepared according to our previously described methods.[37] Briefly, round siliconized cover slides of 8 and 14 mm diameter were prepared by treatment with 2% (v/v) trimethylchlorosilane/$CHCl_3$ solution, followed by baking at 180 °C for 4 h. All materials were dissolved in chloroform with a concentration of 3% (w/v). Subsequently, 10 μL or 20 μL of the solution was added dropwise to a cover slide to form a thin film by evaporation in air. The cover slides were dried under vacuum for 48 h at 25 °C. The cover glasses and microcarriers were placed on culture plates (Costar, Corning, Inc., Corning, NY, USA), sterilized with 75% (v/v) alcohol and UV for 60 min, and then washed with PBS (pH = 7.4) three times.

Cell experiments were performed using mouse pre-osteoblast MC3T3-E1 cells purchased from the Institute of Biochemistry and Cell Biology, Shanghai Institutes for Biological Sciences, Chinese Academy of Sciences. To investigate the effects of the grafting ratio on cell proliferation in 2-D culture, 2×10^4 cells were seeded on the films of different materials (on cover slides of 14 mm in diameter) in 24-well culture plates and cultured with high-glucose Dulbecco's modified Eagle's medium (DMEM; Gibco, Invitrogen) supplemented with 10% fetal bovine serum (Zhejiang Tianhang Biotechnology Co., Ltd, China), 63 mg L^{-1} penicillin (Solarbio, Beijing, China), and 100 mg L^{-1} streptomycin (Solarbio) in a humidified atmosphere of 95% air and 5% CO_2 at 37 °C. The culture medium was changed every 2 days. Cell viability was measured by 3-(4,5-dimethyl)thiazol-2-yl-2,5-dimethyl tetrazolium bromide (MTT; Biosharp, Beijing, China) assays. After culture for 1, 3, and 7 days, 60 μL of MTT solution (5 mg mL^{-1}) was added to each culture well. The cells were continually cultured for another 4 h. During this period, viable cells reduce MTT to formazan pigment, which was then dissolved in 600 μL of dimethyl sulphoxide (DMSO) after the removal of the culture medium. Subsequently, 150 μL of the DMSO solution was transferred to a 96-well culture plate (Costar, Corning). The absorbance at 492 nm was recorded using a microplate reader (Infinite M200; Tecan, Switzerland). Average results were obtained from four parallel samples.

For the following experiments, the microspheres (MHA/PLGA microspheres and PBLG-*g*-MHA microspheres) and thin films of PBLG-*g*-MHA on cover glasses of 8 mm diameter were placed in 48-well culture plates and pretreated by immersion in 300 μL of DMEM for 12 h under a humidified atmosphere of 95% air and 5% CO_2 at 37 °C. In total, 15 mg of microcarrier was used for each well. After the removal of DMEM, 1×10^4 cells per well MC3T3-E1 pre-osteoblast cells were seeded onto the culture plate. After the osteoblasts were cultured on different kinds of microspheres and materials for 1, 3, and 7 days, the groups of microcarriers were transferred to another 48-well cell culture plate and 30 μL of MTT solution (5 mg mL^{-1}) was added to each well. The cells were continually cultured for another 4 h and dissolved in 400 μL of DMSO after the removal of the culture medium. The subsequent test steps were the same as those described above.

Cell morphology and distribution were investigated by fluorescence microscopy after the cells were cultured for 3 days. The cell–microsphere samples were removed from the original culture wells, rinsed with PBS solution three times, and stained with Calcein-AM (Aladdin, China) for 10 min at 37 °C. Subsequently, the samples were rinsed three times with PBS. Nuclear staining was performed using 4′,6-diamidino-2-phenylindole (DAPI; Sigma, USA). The cell–microsphere composites were incubated in DAPI/PBS staining solution (2 μL mL^{-1}) for 1 min at room temperature. Further, the samples were washed three times with PBS. Cell–microsphere samples were observed using the Axio Imager A2 (Zeiss, Germany) fluorescence microscope.

2.6.4 Quantitative real-time PCR. MC3T3-E1 cells cultured on various experimental microspheres and materials were incubated at 7 and 14 days. The expression of osteogenesis-related genes was quantitatively assessed by real-time PCR. Total RNA of cells grown on different groups was extracted using TRIzol Reagent (Invitrogen, Thermo Fisher) according to the manufacturer's instructions. The concentration and purity of RNA were measured using Nanodrop Plates (Infinite M200, Tecan). The mRNAs of all the samples were reverse-transcribed using the PrimeScript RT Reagent Kit with the gDNA Eraser RR047A (TaKaRa, Japan). The expression of osteogenic genes was quantified using SYBR Premix Ex Taq RR420A (TaKaRa, Japan). Gene-specific primers targeting glyceraldehyde-3-phosphate dehydrogenase (*GAPDH*), anti-runt-related transcription factor 2 (*Runx 2*), osteopontin (*OPN*), osteocalcin (*OCN*),

Table 2 Fine sphere ratio of microcarriers fabricated with different grafting amounts and solution concentrations

	Graft amounts			
Solution concentration	11.82%	22.38%	33.12%	50.30%
1%	0%	0%	15%	75%
3%	0%	65%	88%	96%
5%	7%	49%	52%	28%

and collagen-I (*Col-I*) were designed and are shown in Table 3. Real-time PCR was performed using the Stratagene Mx3005P Real-time qPCR System (Agilent Technologies Inc., USA) and the gene expression levels were obtained using the threshold cycles (Ct). Relative transcript quantities were calculated using the ΔΔCt method. *GAPDH* was used as a reference gene and was amplified along with the target genes from the same cDNA samples. The difference in the Ct value of the sample relative to *GAPDH* was defined as ΔCt. The difference between ΔCt of the control group cells and the ΔCt of the cells grown on experimental groups was defined as the ΔΔCt. The fold change in gene expression is expressed as $2^{-\Delta\Delta Ct}$.

3. Results and discussion

Compared to the currently used polyesters (*i.e.*, PLA and PLGA), polypeptides (*i.e.*, poly(γ-benzyl-L-glutamate)) have been reported to possess better biocompatibility and specific bioactivities.[26,27,32] The aim of this study was to obtain biodegradable and biocompatible microcarriers consisting of MHA nanoparticles and poly(γ-benzyl-L-glutamate) by the *in situ* ring opening polymerization of BLG-NCA on the surface of MHA using the O/W solvent-evaporation method. Traditionally, the preparation of composite materials includes two steps. Surface-modified MHA is firstly synthesized, then the product is blended with a kind of polymer matrix. Usually, multiple kinds of polymers are used in these composite microcarriers, which might result in complicated physiological issues *in vivo*, and, mostly, the matrix materials do not have any bioactivities. In the present study, PBLG-*g*-MHA microcarriers with high graft amounts of PBLG were directly fabricated without the addition of other biodegradable polymers, such as PLGA or PCL. Thus, the preparation route of the composite materials was simplified and the intrinsic properties of HA and PBLG could be effectively improved. This method provides a new strategy for preparing multifunctional composite materials. The preparation route for the PBLG-*g*-MHA microcarriers is shown in Scheme 1.

3.1 Synthesis and characterization of PBLG-*g*-MHA

3.1.1 Characterization of MHA. Mesoporous hydroxyapatite was successfully synthesized according to XRD and N_2 adsorption/desorption isotherms analyses, which are shown in Fig. 1(b) and Table S1 (ESI†). It can be clearly seen from Fig. 1(b) that synthesized MHA showed characteristic diffraction peaks, and no peaks of other calcium phosphate phases were detected. As shown in Table S1 (ESI†), MHA has a BET surface area (S_{BET}) of 59.099 $m^2\ g^{-1}$, average pore size (d_P) of 27.282 nm and pore volume (V_P) of 0.437 $cm^3\ g^{-1}$, which are much higher than that of nano-HA. These results clearly indicated that mesoporous HA was successfully synthesized.

3.1.2 NMR and FT-IR analysis. As shown in Fig. S1 (ESI†), the successful synthesis of BLG-NCA could be confirmed through ^{1}H-NMR analysis. The original MHA was pre-treated with APS to obtain MHA-APS, which has amino groups on the surface. The surface amino groups of MHA were used to initiate the ring opening polymerization of BLG-NCA.

The reaction was continued in dried dioxane at 25 °C. During the ring opening polymerization of BLG-NCA, trace quantities of NCA molecules might be initiated by the possible existence of APS separated from the surface of MHA-APS or other substances existing in the reaction system. Thus, physisorbed PBLG could be generated and the free PBLG chain could contribute to the direct preparation of the PBLG-*g*-MHA microspheres. We thoroughly washed the product by repeated dissolution and dispersion, ultrasonic treatment and centrifugation to remove the physisorbed PBLG. Successful preparation of PBLG-*g*-MHA was confirmed by FTIR, as shown in Fig. 1a. In comparison with the original MHA, PBLG-*g*-MHA showed peaks at 1735 cm^{-1}, attributed to the carbonyl bond on the side chain of PBLG, and at 1652 and1547 cm^{-1}, indicating the existence of amide groups, a characteristic functional group of polypeptides. The peak at 3290 cm^{-1} represented the N–H stretching vibration. Peaks at 697 and 749 cm^{-1} confirmed the existence of benzene rings, which further indicated that PBLG was successfully grafted onto MHA.

3.1.3 XRD analysis. X-Ray diffraction is able to reflect the molecular and crystal structure of a crystalline material. As shown in Fig. 1b, the characteristic diffraction peaks of all the PBLG-*g*-MHA products were almost the same as the XRD patterns of pure MHA, such as the diffraction peaks at (002), (211), (310), (222), (213) and (004). Although the above-mentioned diffraction peak intensity declined, this was mainly due to the increase of polymer content. This result demonstrated that the surface modification procedure did not affect the crystallographic properties of the pure MHA nanocrystals.

Table 3 Primary sequences of *GAPDH*, *Runx 2*, *OPN*, *OCN* and *Col-I*

Gene	Forward primer sequence (5′–3′)	Reverse primer sequence (5′–3′)
GAPDH	TGAACTAACACAGAGGAGGATCAG	GCTTAGGGCATGAGCTTGAC
Runx 2	GCCGGGAATGATGAGAACTA	GGACCGTCCACTGTCACTTT
OPN	TCAGGACAACAACGGAAAGGG	GGAACTTGCTTGACTATCGATCAC
OCN	AAGCAGGAGGGCAATAAGGT	TTTGTAGGCGGTCTTCAAGC
Col-I	CGCTGGCAAGAATGGCGATC	ATGCCTCTGTCACCTTGTTCG

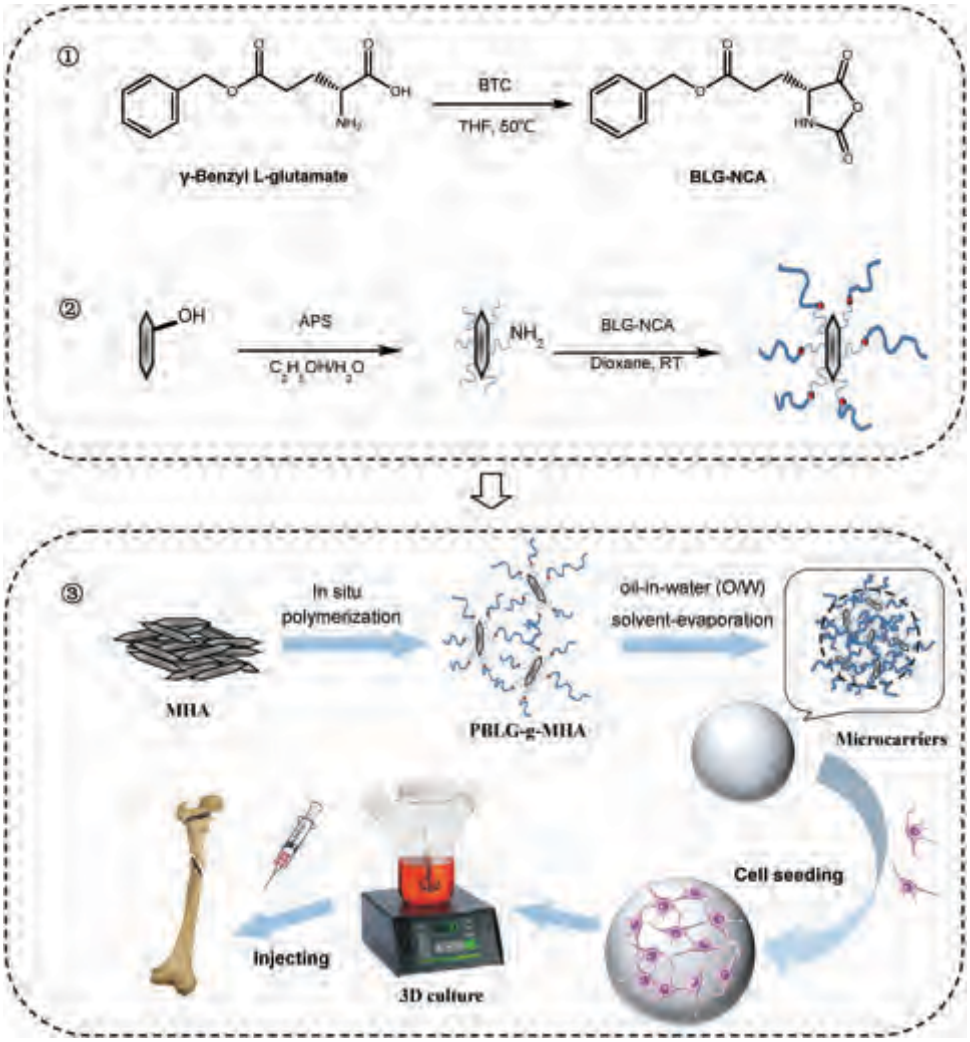

Scheme 1 Preparation route of PBLG-*g*-MHA microcarriers through *in situ* polymerization of poly(γ-benzyl-L-glutamate) (PBLG) on mesoporous hydroxyapatite (MHA) and their applications in cell expansion for bone tissue engineering.

3.1.4 TGA analysis. The amount of grafted PBLG was measured by TGA. The detailed results are shown in Fig. 1c and Table 1. As shown in Table 1, by adjusting reaction conditions, the surface-modified MHA with different amounts of grafted PBLG could be obtained. The graft amount of 1.80 wt% was because of the APS attached to the surface of MHA. When different amounts of PBLG were grafted onto the surface of MHA, the weight loss was obviously different. By varying the feed ratio, PBLG-*g*-MHA samples with different amounts of grafted material, ranging from 11.82 wt% to 50.30 wt%, were prepared.

3.1.5 Water contact angle. An increase in the hydrophilicity of materials facilitates the attachment and proliferation of cells; accordingly, hydrophilic materials are desirable for successful cell growth and tissue regeneration. Thus, static water contact angle tests were conducted to investigate the surface hydrophilicity of the PBLG-*g*-MHA materials. HA is a well-known hydrophilic biomaterial and PBLG is hydrophobic. Therefore, as the amount of surface PBLG increased, the hydrophobicity of the PBLG-*g*-MHA composite material is expected to increase. As shown in Fig. 2, the results clearly indicated that for samples with the same amount of PBLG, as the concentration of the PBLG-*g*-MHA/$CHCl_3$ solution increased, the water contact angle increased slightly. For the same concentrations, as the amount of PBLG increased, the water contact angle increased markedly. Traditionally, if the liquid drop spreads on the sample surface, corresponding to a contact angle of less than 90 degrees, the material is called hydrophilic. Most of the obtained samples were hydrophilic, except the PBLG-*g*-MHA samples with a graft amount of 50.30 wt% and solution concentrations of 3% and 5% (w/v). But even for the most hydrophobic material, the contact angle was only 96.52 degrees. From this point of view, the PBLG-*g*-MHA microspheres would provide an effective matrix for cell attachment and growth.

3.2 Fabrication and characterization of PBLG-*g*-MHA microcarriers

3.2.1 Overview of microsphere formation. The formation mechanism of the PBLG-*g*-MHA microspheres without any other biodegradable polymer matrix could be explained by

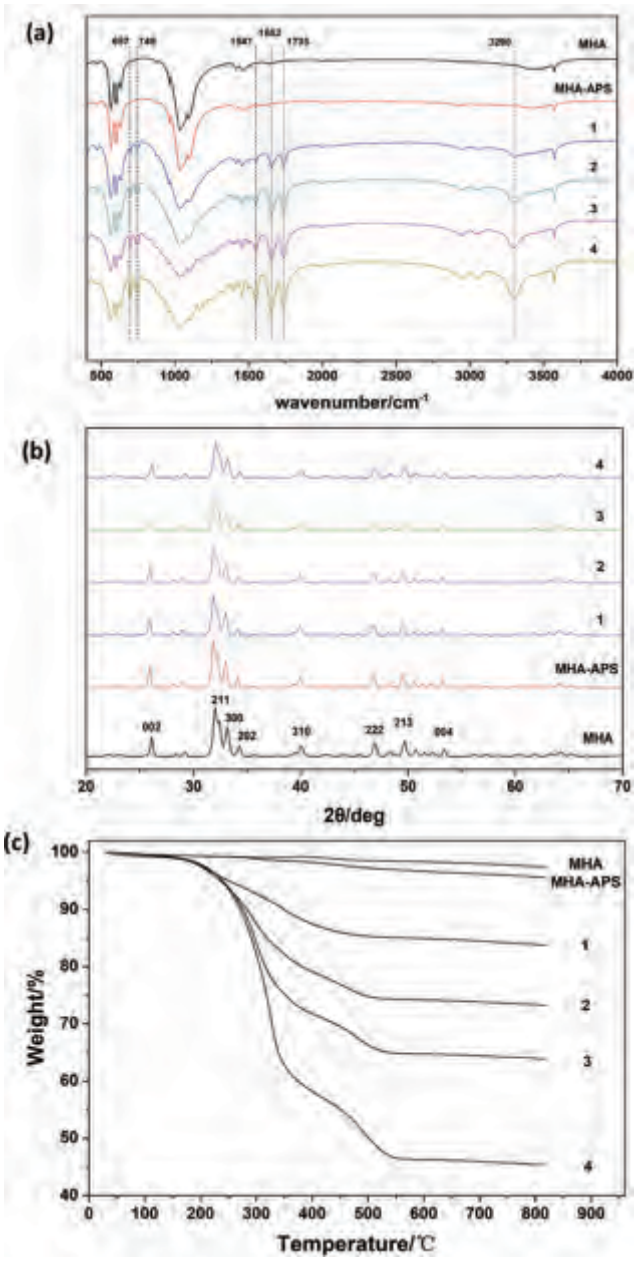

Fig. 1 FT-IR spectra (a), XRD patterns (b), and TGA curves (c) of MHA, MHA-APS, and PBLG-*g*-MHA (1 to 4).

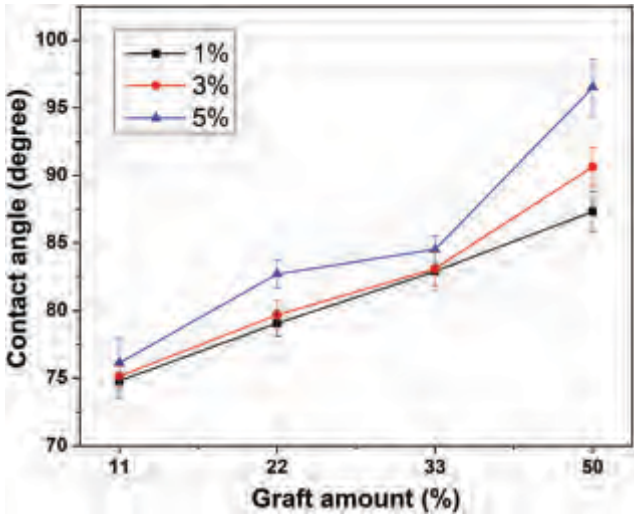

Fig. 2 Contact angle analysis of PBLG-*g*-MHA with different graft amounts (11%, 22%, 33%, and 50%) and solution concentrations (1%, 3%, and 5%).

polymer chain entanglement and organic solvent evaporation, and it is schematically shown in Scheme 1. The PBLG-*g*-MHA/$CHCl_3$ phase (oil phase) was cut into small spherical droplets by shear force under vigorous stirring when it was added to the PVA/H_2O solution (water phase). PVA is a water-soluble macromolecule used to prevent the coalescence of droplets under continuous stirring. Thus, the concentration of PBLG-*g*-MHA and the graft amount of PBLG-*g*-MHA are the most likely factors affecting microsphere formation. To investigate the effects of these two parameters, a series of experiments under various conditions (including three different concentrations of the PBLG-*g*-MHA/$CHCl_3$ solution and four different graft amounts of PBLG-*g*-MHA) was conducted to explore the effects on microsphere formation and morphology. The samples were examined by SEM and statistical analyses with Image J software.

In general, an increasing amount of PBLG resulted in the better formation of spheres (as shown in Fig. 3 and fine sphere ratios in Table 2). We define the fine sphere ratio as the difference in two orthogonal diameters of a single microsphere of less than 10%. An appropriate concentration led to the formation of regular and fine microparticles (Fig. 3g and h), while a low concentration resulted in the failed fabrication of microspheres (Fig. 3a and b) and a high concentration induced particle aggregation (Fig. 3l). Both the graft amount and concentration had substantial effects on the shape and diameter of microspheres. For all three concentrations of the solution, almost no spheres were obtained in the groups with a graft amount of 11.82 wt% (Fig. 3a, e, and i). The amount of PBLG on the MHA surface was too low and polymer chain entanglement could not be achieved. Thus, under vigorous stirring, irregular particles were obtained. For each concentration, a lower graft amount (11.82 wt%) resulted in spheres that were not uniform in shape, and breakage was frequently observed (Fig. 3(a), (b), (e), and (i)). With a higher amount of PBLG ($\geq$22.38 wt%), the spheres were more orbicular. When the graft amount was sufficiently high (33.12 wt% and 50.30 wt%), the spheres maintained their integrity, indicating that the entanglement of each small piece of a droplet was sufficient and spherical PBLG-*g*-MHA microspheres could be obtained. With respect to the concentration of PBLG-*g*-MHA/$CHCl_3$ solution, a low concentration would lead to particles with irregular shapes and rugged surfaces. At a relatively low concentration of the composite solution, the droplet was cut into small pieces under vigorous stirring, and these fragments do not recombine with sufficient frequency. Under a relatively high concentration, microspheres with oval shapes and coalescent spheres were observed. A higher concentration of the solution would result in a higher collision probability. With the same

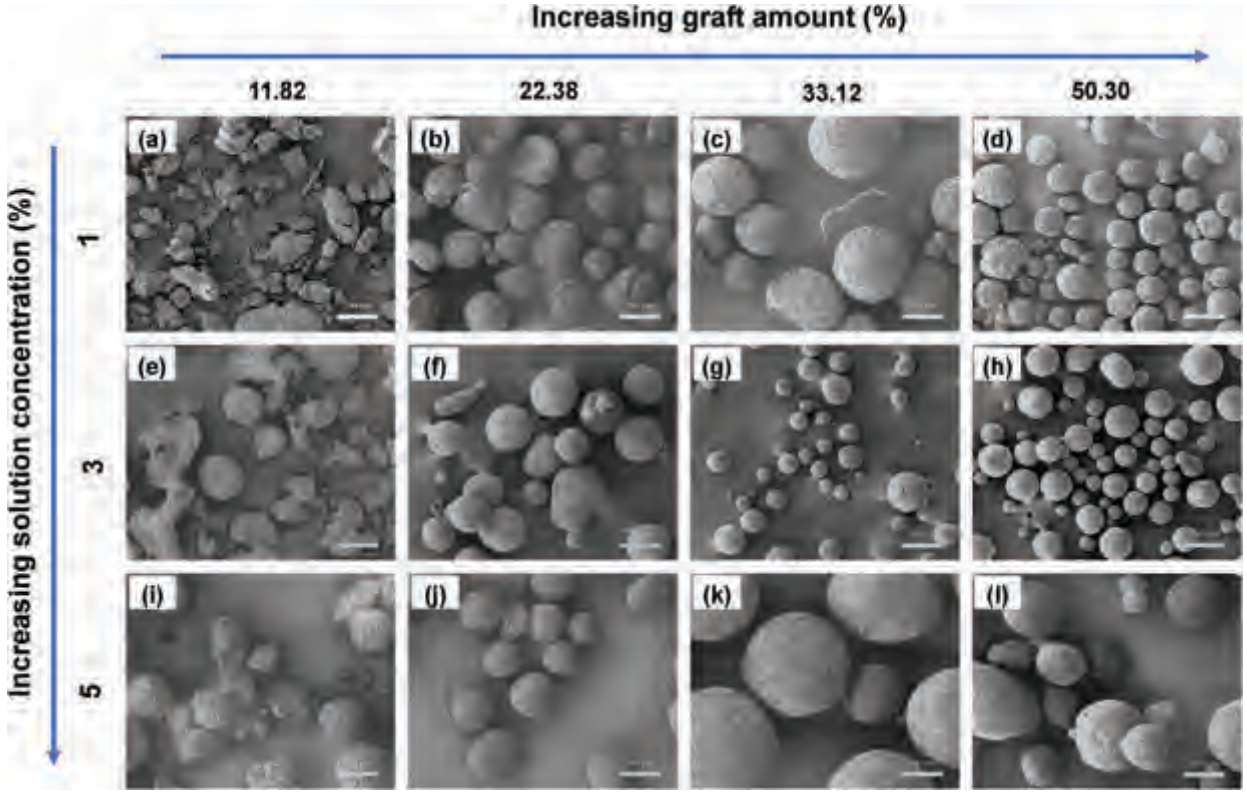

Fig. 3 SEM micrographs of PBLG-*g*-MHA microcarriers. The graft amounts were 11.82%, 22.38%, 33.12%, and 50.30%, and the solution concentrations were 1%, 3%, and 5%. Scale bars represent 200 μm.

shear force, the oil phase was cut into spherical droplets and the separated droplets could easily aggregate. Thus, oval and irregular microspheres were formed. Accordingly, these two factors have a strong influence on the morphology of the PBLG-*g*-MHA microspheres.

The average diameter and size distribution of microcarriers are shown in Fig. 4. As shown in Fig. 4a, the average diameters of all spheres were between 100 and 300 μm and they could be substantially affected by both the graft amount and concentration. The sizes of microspheres for a medium concentration (3%, w/v) were smaller than those observed for a low concentration (1%, w/v) and a high concentration (5%, w/v). For the low and medium concentrations (1% and 3%, w/v), the sizes of microspheres seemed to decrease as the graft amount increased to more than 33.12 wt%. However, for a high concentration (5%, w/v), the sizes increased with an increase of the graft amount. It is possible that the lower viscosity for the groups with low concentrations resulted in looser microstructures and poor sphericity, and a higher viscosity for the groups with high concentrations resulted in increased binding and fusion. Combining the size distribution (Fig. 4b) and morphology (Fig. 3), the microspheres in the groups with a graft amount of 50.30 wt% in a low concentration, 33.12 wt% and 50.30 wt% in a medium concentration, and 22.38 wt% in a high concentration exhibited more uniform sizes and better sphericity. Among these, the microspheres in the groups with graft quantities of 33.12 wt% and 50.30 wt% in a medium concentration (3%, w/v) were the best candidates and therefore were used in subsequent analyses of cell growth and proliferation owing to their high surface regularity.

The differences in the surface topography and element contents between the two kinds of microcarriers with graft amounts of 33.12 wt% and 50.30 wt% were analyzed by SEM and the results are summarized in Fig. 5. A higher amount of PBLG was associated with spheres that were rounder and glossier (Fig. 5a-1, a-2 and b-1, b-2), but greater surface roughness was observed in the high-magnification images (Fig. 5a-3 and b-3). Although a porous surface was observed for both groups, the group with the higher amount of PBLG exhibited more and larger micropores on the surface. This was mainly explained by the greater plasticity of PBLG-*g*-MHA for the formation of spheres as the amount of PBLG increased. The micropores might result from solvent removal during the preparation of microspheres under continuous stirring; their quantities and sizes would be associated with the solvent evaporation rate. Surface roughness is reported to be beneficial for cell attachment and proliferation on microspheres.[38] As shown in Fig. 5(c) and (d), through SEM and EDX analysis, elements of Ca, P and N could be detected. This indicated that HA exposed on the surface of microcarriers, and the amido bond (peptide bond) of PBLG might better mimic the natural ECM structure.

Based on these results, the microspheres with graft amounts of 33.12 wt% and 50.30 wt% obtained at a concentration of 3% (w/v) presented the best spherical shape, and therefore might

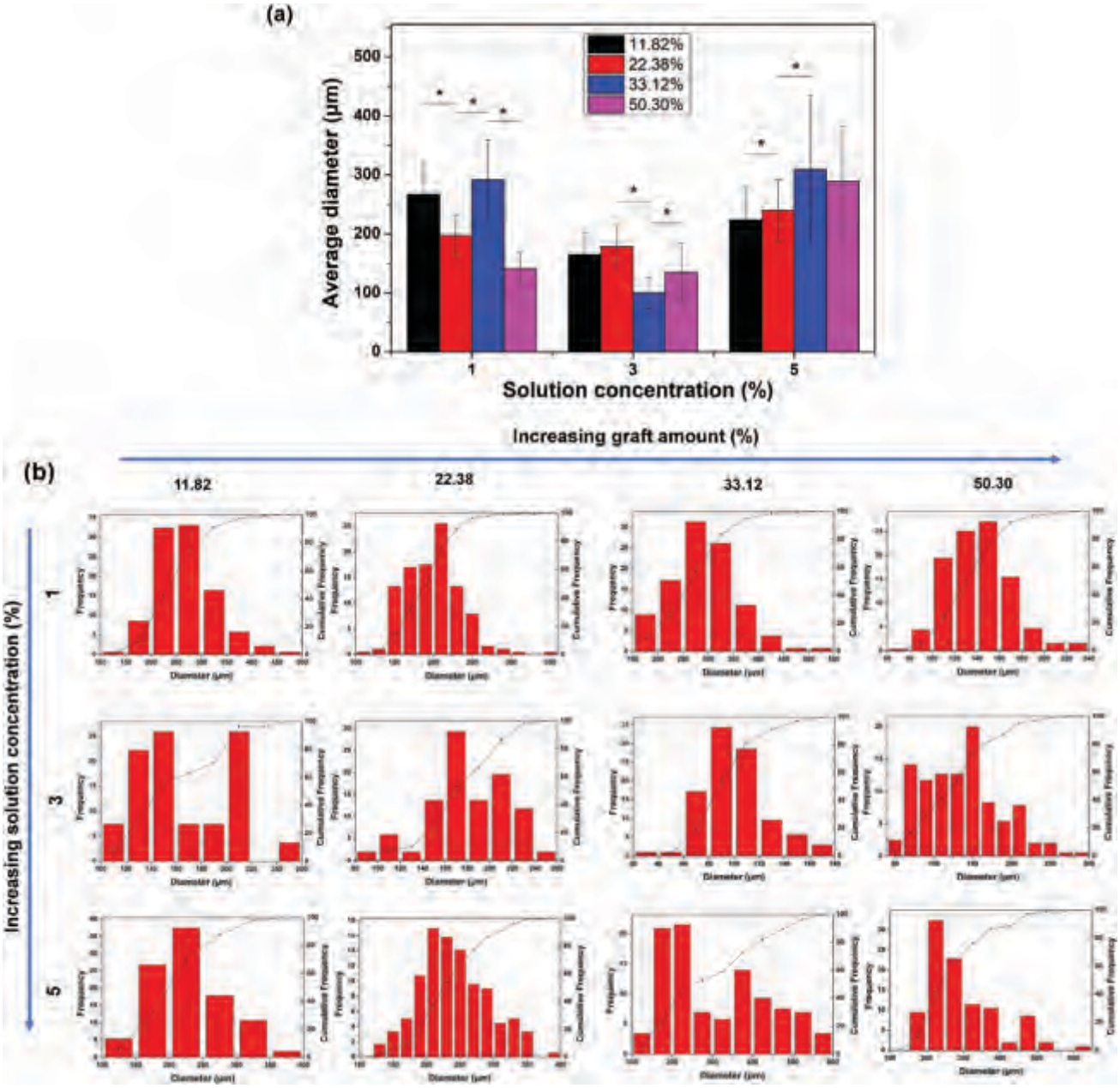

Fig. 4 Statistical analysis of the average diameter (a) and size distribution (b) of microcarriers fabricated using different graft amounts (11.82%, 22.38%, 33.12%, and 50.30%) and solution concentrations (1%, 3%, and 5%).

be suitable to act as microcarriers for osteoblasts. Thus, the microspheres employed in subsequent biological experiments were prepared using a solution concentration of 3% (w/v) and graft amounts of polymers of 33 wt% and 50 wt%. For the control group MHA/PLGA microspheres with PLGA contents of 33 wt% and 50 wt%, as shown in Fig. S2 (ESI†), there were no significant differences in their size, spherical shape and surface morphology compared to the PBLG-*g*-MHA microcarriers. As shown in Fig. S2(c) and (d) (ESI†), elements of Ca and P could also be detected, as in Fig. 5(c) and (d).

3.2.2 *In vitro* biodegradation study. Cell expansion is closely related to the micro-environment of the substrate, especially for microcarriers of biodegradable polymers, such as changes in pH, surface morphology and surface elements, due to their biodegradation. Fig. 6(A) shows the patterns of pH variation for the PBLG-*g*-MHA microspheres (33 wt% and 50 wt% graft ratios) incubated in PBS as a function of incubation time. The pH values of the incubation solution for both microcarriers decreased gradually but were maintained at 7.1–7.3 over the whole incubation period. Additionally, the pH value of the microcarriers with a grafting ratio of 33 wt% was slightly higher before 5 days and then became lower than that of the microcarriers with a ratio of 50 wt%. This was mainly because a lower grafting ratio of PBLG indicated a low molecular weight

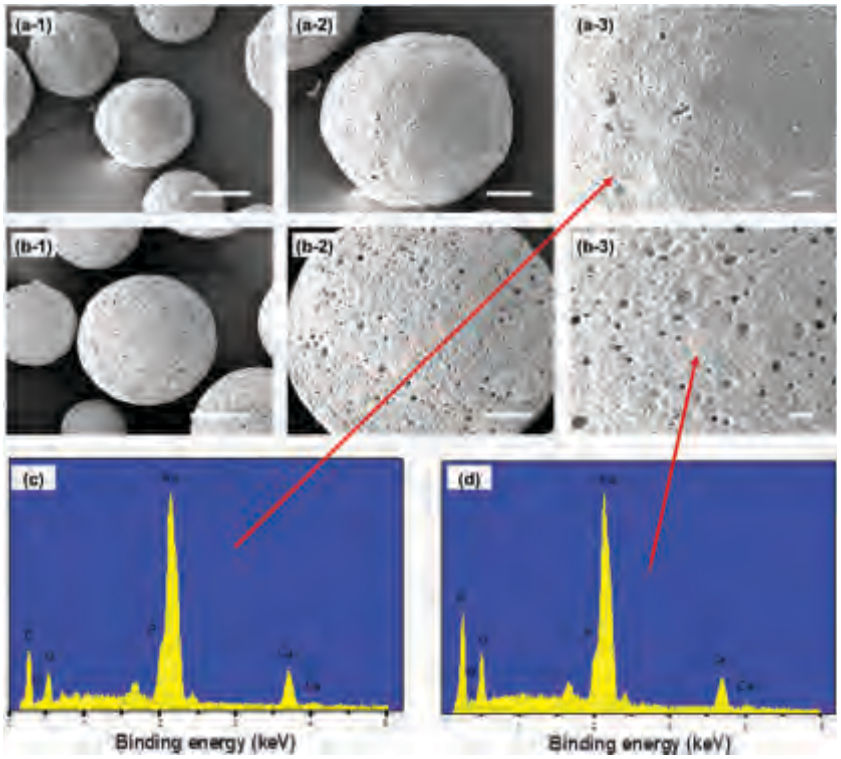

Fig. 5 SEM micrographs and EDX analysis of PBLG-*g*-MHA microcarriers with graft amounts of 33.12% (a and c) and 50.30% (b and d) and solution concentrations of 3%. (2) and (3) are the amplified micrographs of (1). The scale bars represent 50 μm (1), 20 μm (2), and 10 μm (3). EDX curves (c and d) showed the element contents of P and Ca on the surfaces of the microcarriers (a and b), respectively.

and thus easy degradation. The degradation behavior of the PBLG-*g*-MHA microspheres might be related to the degradation of PBLG and HA. It is possible that the pH of the incubation solution decreases during the degradation of PBLG, but this trend may be weakened because the acid degradation product could be neutralized by the alkaline ions released from the HA nanoparticles. This is quite favorable for the utilization of PBLG-*g*-MHA microcarriers as vehicles of cell production and for *in vivo* implantation, inducing less substantial inflammatory responses. The slight differences in pH changes between 33 wt% and 50 wt% might be explained by the difference in the ratio of PBLG to HA. A higher HA content will result in the more rapid degradation of microspheres.

The SEM micrographs and EDX analysis of the above-mentioned PBLG-*g*-MHA microspheres are shown in Fig. 6(B) and 6(C), respectively. Obvious surface defects were observed on the 33 wt% PBLG-*g*-MHA microspheres after 1 week of incubation, indicating the degradation of the PBLG polymer or HA. This led to surface roughness, and the roughness increased with the incubation time, but the sphere structure was maintained in the initial state. In contrast, the groups with 50 wt% PBLG showed little degradation after 1 week of immersion and infrequent breakage after 2 weeks. During the whole degradation period, the 33 wt% microsphere group exhibited a faster degradation rate than that of the 50 wt% group. The 33 wt% microspheres had a relatively high content of HA (the inorganic part of the microspheres), resulting in faster degradation. On the other hand, they had a lower content of organic matrix (PBLG) and they degraded easily owing to the loose microstructure after immersion in PBS. There were almost no broken microspheres within 28 days of the degradation test, indicating that the PBLG-*g*-MHA microspheres of both 33 wt% and 50 wt% are suitable for cell expansion and tissue engineering. Besides, the elemental analysis results (Fig. 6C) revealed that over the whole degradation period, the surface amounts of elements of Ca and P did not change obviously, which suggested the homogeneity of the PBLG-*g*-MHA microcarriers. Thus, during the degradation of microspheres, the surface would always be beneficial for cell proliferation.

3.3 Biological assessment

3.3.1 Cell proliferation. Efficient expansion of osteoblasts would be highly beneficial for bone tissue engineering in clinical settings. Expansion depends on the biocompatibility of the materials, the structure of substrates, and the culture system in 2-D or 3-D. Before the cytological assessments of the PBLG-*g*-MHA microspheres, cell viability assay of PBLG-*g*-MHA raw materials with different graft ratios was performed using the MTT method, and the results are shown in Fig. 7a. The cell counts for all the groups increased obviously from 3 days to 7 days. At 1 day, the cell viability was slightly higher in MHA/PLGA and PBLG-*g*-MHA/PLGA (11 wt%) and lower in PLGA and MHA-APS/PLGA, but there were no significant differences among groups. On the third day, similar results were obtained, except the PBLG-*g*-MHA/PLGA (11 wt%) group exhibited higher cell counts compared to those of the non-grafted group of

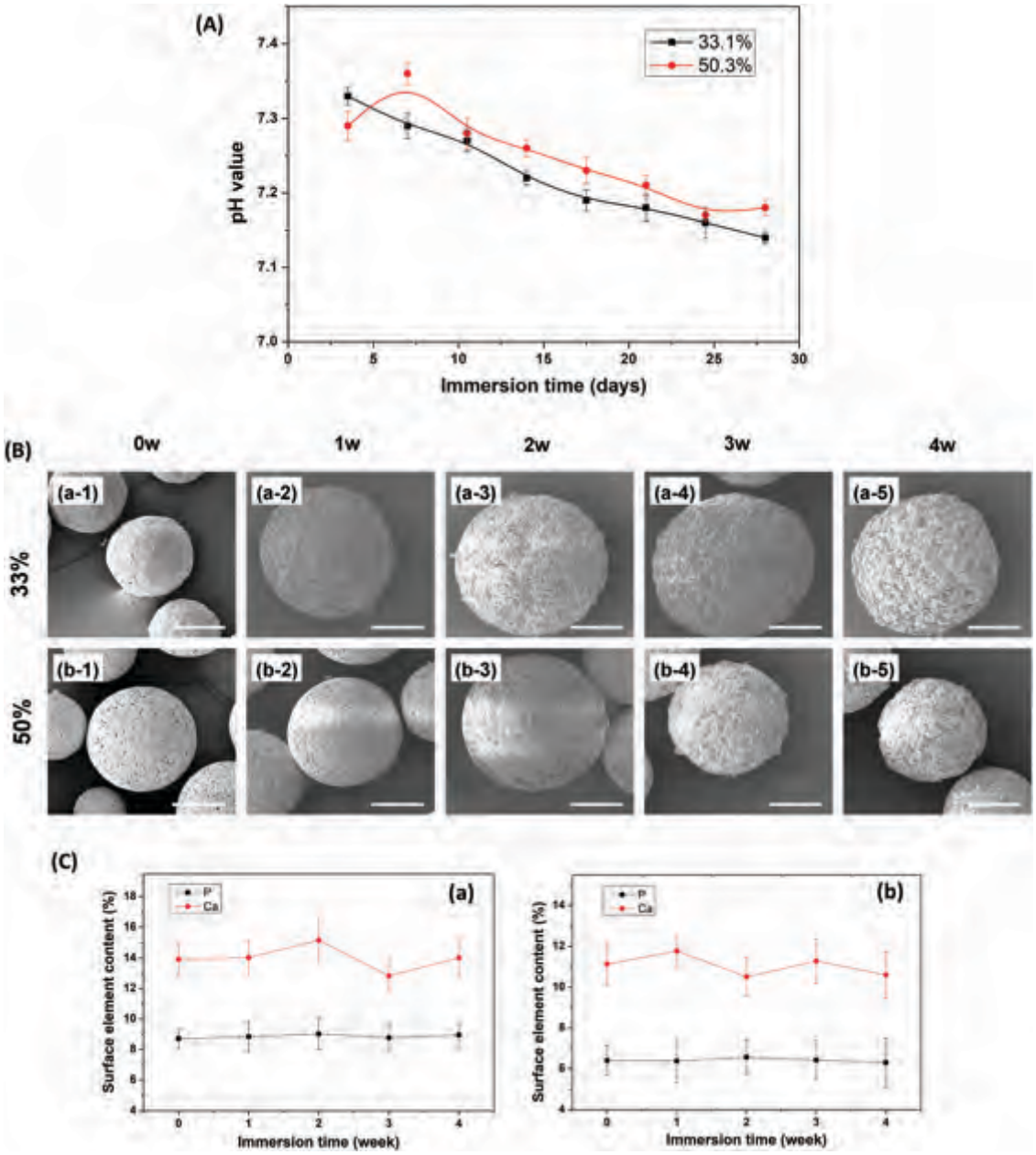

Fig. 6 Summary of *in vitro* degradation tests of PBLG-*g*-MHA microspheres. (A) pH values of the incubation solutions of PBLG-*g*-MHA microspheres in the *in vitro* degradation test. (B) SEM images show the surface topography changes of the PBLG-*g*-MHA microspheres with graft amounts of 33% (a) and 50% (b) immersed in PBS for different durations: (1) before the degradation test; (2) after 1 week; (3) after 2 weeks; (4) after 3 weeks; (5) after 4 weeks. Scale bar: 50 μm. (C) EDX analysis shows the element contents of Ca and P on the surfaces of microspheres with the graft amounts of 33% (a) and 50% (b).

MHA/PLGA ($p < 0.05$), which demonstrated that the MHA surface grafted with PBLG exhibited improved cell attachment and proliferation. However, cell attachment decreased slightly with increasing graft amounts. After 7 days, a high amount of PBLG (PBLG-*g*-MHA 22 wt%, 33 wt%, and 50 wt%) demonstrated better cell expansion ability and biocompatibility compared to those of the other groups, but there were no significant differences among the three groups. We deduced that when the amount of PBLG on the surface of MHA was sufficiently high, the influence of graft amount on cell proliferation was small, despite the existence of glutamate, which seems to participate in bone cell signaling and intercellular communication.[39] Thus, the microcarriers of PBLG-*g*-MHA with graft ratios of 33 wt% and 50 wt% were selected for subsequent experiments based on their fabrication properties and influence on cell viability.

Fig. 7b shows the viability of MC3T3-E1 pre-osteoblast cells on the films and microcarriers of PBLG-*g*-MHA (33 wt% and 50 wt%), as determined by MTT assays. The biological function of the PBLG-*g*-MHA microspheres for 3-D culture was compared to that of films for 2-D culture. A lower cell viability on the microcarrier groups was observed at 1 day compared to that of

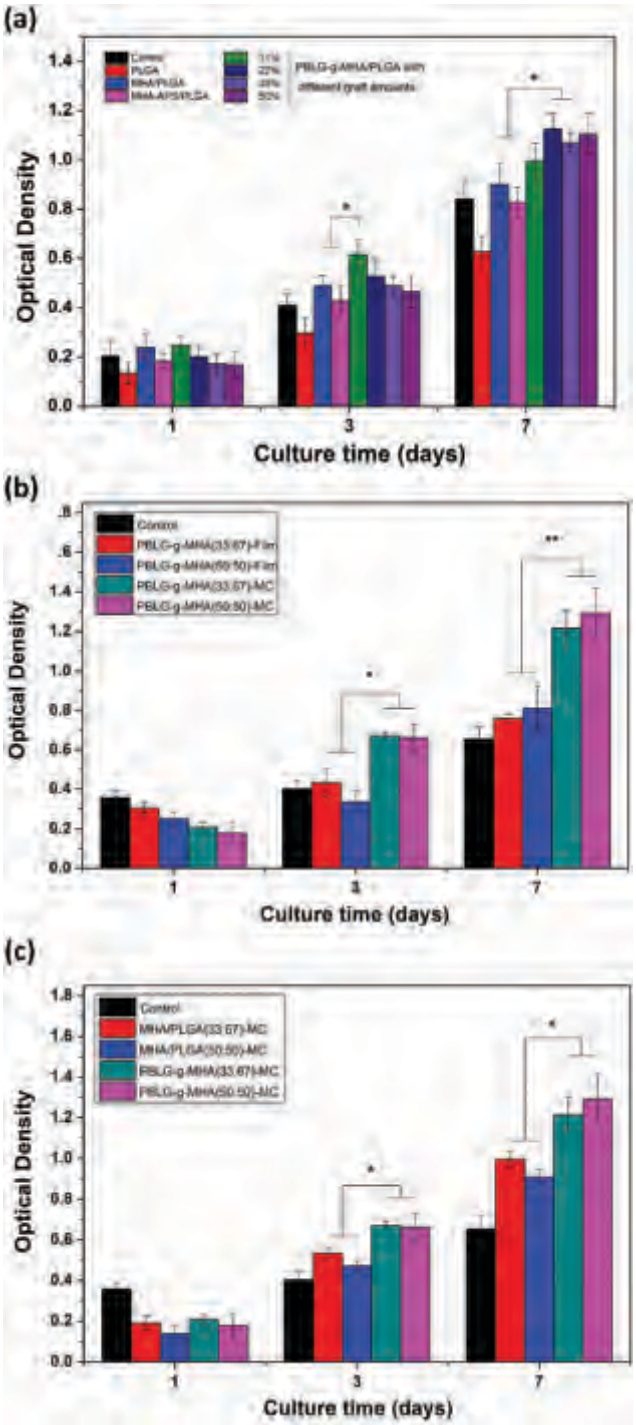

Fig. 7 MTT assay of MC3T3-E1 cells grown on (a) the PBLG-*g*-MHA film with different graft amounts, (b) the PBLG-*g*-MHA film and microcarriers with graft amounts of 33% and 50%, and (c) MHA/PLGA microcarriers and PBLG-*g*-MHA microcarriers with the same organic component ratio of 33% and 50% at different culture times.

the films. For the groups of 3-D microspheres, the spaces between microspheres led to lower cell adhesion compared to that on the films at the initial period. Subsequently, cells cultured on the microcarriers exhibited greater proliferation ability compared to that of cells on the films at 3 and 7 days, indicating that the microcarriers were quite suitable for cell expansion owing to their high surface areas.

MHA/PLGA microcarriers and PBLG-*g*-MHA microcarriers were also compared with respect to cell viability using MTT tests, as shown in Fig. 7c. As a supporting matrix for cell expansion, the biological properties of materials play a key role in the promotion of cell adhesion and growth.[40] Among the MHA/PLGA and PBLG-*g*-MHA microcarriers, there were no substantial differences in cell proliferation at 1 day, and all of the microsphere groups exhibited lower cell numbers compared to that of the control group. However, at 3 and 7 days, the PBLG-*g*-MHA microcarrier groups showed higher cell viability compared to that of the MHA/PLGA microcarriers, indicating that PBLG possesses better biological properties than PLGA. There were no significant differences in cell numbers among the PBLG-*g*-MHA microcarriers with different amounts of PBLG. This can be explained by the results of the MTT assays for PBLG-*g*-MHA with different graft amounts. In addition, the cell proliferation assay was conducted by traditional cell culture plates, and therefore the aim of cell culture using microcarriers was not fully achieved. In this study, PBLG-*g*-MHA microcarriers were effectively utilized to obtain better cell proliferation, facilitate cell–cell interactions, and rebuild the natural 3-D environment.

3.3.2 Cellular morphology and distribution. The morphology and distribution of MC3T3-E1 cells grown on different microspheres at 3 days was observed using a fluorescence microscope after Calcein-AM live cell staining and DAPI nuclear staining. The Calcein-AM staining showed the cellular morphology, and the nuclear staining indicated the number of cells grown on the surfaces of microcarriers. As detected by fluorescence staining, the PBLG-*g*-MHA microspheres (Fig. 8c and d) were almost completely covered with osteoblasts, and fewer cells were found on the MHA/PLGA microspheres (Fig. 8a and b). The MC3T3-E1 cells (bright green dots) aggregated and were densely and evenly distributed on both PBLG-*g*-MHA microspheres. This is consistent with the results of the cell proliferation assay. Furthermore, the cells grew much better on the PBLG-*g*-MHA microspheres than on the corresponding microspheres not only with respect to density, but also cell morphology, and they exhibited greater spreading, indicating greater cell attachment and expansion for the PBLG-*g*-MHA microspheres. These results further supported the role of microcarriers and PBLG in promoting the attachment and proliferation of osteogenic cells.

3.3.3 Quantitative real-time PCR. The main stages of osteogenic cells after seeding on a substrate are cell adhesion, spreading, proliferation, differentiation, ECM secretion and mineralization.[41,42] These stages are regulated by various genes during each period. The results of the *in vitro* proliferation assay of pre-osteoblast cells suggested that the PBLG-*g*-MHA microspheres are quite suitable to obtain sufficient numbers of cells. However, the influence on differentiation after cell seeding and proliferation was unclear. Therefore, the expression levels of several osteogenic genes (*Runx 2*, *OPN*, *OCN*, and *Col-I*) in MC3T3-E1 pre-osteoblast cells cultured on PBLG-*g*-MHA

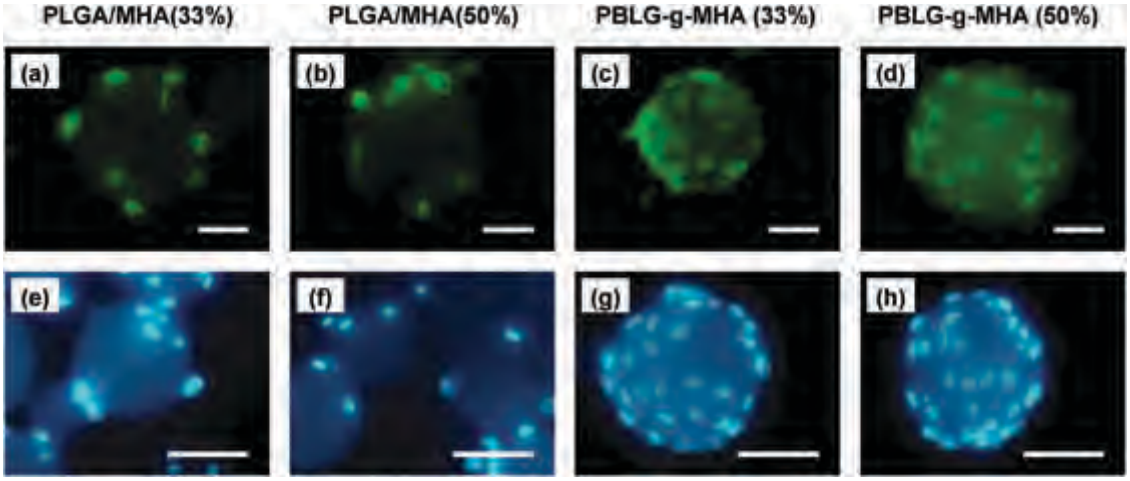

Fig. 8 Fluorescence micrographs of MC-3T3 E1 cells grown on microcarriers of MHA/PLGA (a, b, e, and f) and PBLG-*g*-MHA (c, d, g, and h) for 3 days. Cells were stained with Calcein-AM (a–d) and DAPI (e–h). Scale bar: 100 μm.

microcarriers and the corresponding control groups (MHA/PLGA microcarriers and PBLG-*g*-MHA films) for 7 and 14 days were quantitatively analyzed by real-time PCR and the results are summarized in Fig. 9. *Runx 2* is expressed at the early stage of differentiation. *OPN* expression could be observed after the middle stage and *OCN* is expressed during late differentiation. The *Col-I* gene is first expressed during the initial period of ECM production.[41,43,44] The expression levels of *Runx 2* and *OPN* were higher on the films and microcarrier groups of PBLG-*g*-MHA than on the MHA/PLGA microcarriers and the glass group at 7 days, and the difference in *OPN* between 33 wt% PBLG-*g*-MHA microcarriers and 33 wt% MHA/PLGA microcarriers was statistically significant ($p < 0.05$). At 14 days, the differences in *Runx 2* and *OPN* between the PBLG-*g*-MHA microcarrier groups and other groups decreased, and there were no significant differences among groups ($p > 0.05$). However, the expression levels of *OPN* on material groups were still significantly higher than those of the glass group. At 7 days, the expression levels of *OCN* on all the microcarriers were similar but were significantly lower than the expression levels on the 2-D substrates ($p < 0.05$). For *Col-I*, there were no significant differences among the groups. The expression levels of *OCN* and *Col-1* clearly increased in all the material groups over 14 days. In particular, the expression on PBLG-*g*-MHA microcarriers was significantly higher than that on MHA/PLGA microcarriers. The natural bone matrix is mainly composed of collagens (mainly *Col-I*) and HA nanocrystals (nHA). *OCN* is viewed as a marker for bone formation because it is a specific protein expressed during osteogenic matrix maturation.[45] The real-time PCR results showed that the expression levels of bone-specific maturation genes (*i.e.*, *OCN* and *Col-1*) for the two PBLG-*g*-MHA microsphere groups were obviously increased compared to their expression in other groups, indicating the abilities of some chemical factors to enhance the differentiation of osteogenic cells and bone formation. HA has effects on bone binding and osteoconductivity.[46] Additionally, the peptide bond of PBLG was supposed to mimic the natural protein structure and thus provide a suitable interface for seeded cells.[47] Thus, the increased gene expression levels on PBLG-*g*-MHA microspheres might have resulted from the synergetic bioactivities of HA and PBLG.

In general, biodegradable and bioactive microcarriers with specific functions for improved cell proliferation and osteogenic differentiation were successfully prepared using *in situ* polymerized PBLG-*g*-MHA. Traditionally, inorganic biomineral materials are blended with biodegradable polymers to prepare composite microcarriers.[48] Considering the specific function of glutamate in bone cell signaling and intercellular communication,[26] PBLG is usually employed for bone materials by mixing with other polymers or surface modification methods.[30,32] The composite material systems need other biodegradable polymers (such as PLA and PLGA) as a matrix. In the present study, high graft amounts of PBLG-*g*-MHA fabricated by the *in situ* polymerization of BLG-NCA on MHA nanoparticles could be directly employed to prepare biodegradable and biocompatible microcarriers, without the addition of any other polymers. The intrinsic properties of PBLG, a polypeptide, provided better processing and plasticity, without any non-essential components, like PLGA. The polymer chain entanglement of PBLG has the obvious advantage of providing a stable structure of PBLG-*g*-MHA microcarriers, even after 4 weeks of degradation. The gradually increased surface roughness of microcarriers was caused by the degradation of PBLG or MHA, which is known to support protein adsorption and cell adhesion.

The ability of cells to attach and grow on the surface of microcarriers depends on the chemical composition and surface properties of microcarriers.[8] The improved cell growth and differentiation of osteoblasts on PBLG-*g*-MHA microcarriers in this study may mainly result from their components (PBLG or MHA). The peptide bond of PBLG may mimic the natural ECM structure to provide a suitable surface for cells seeded on the microspheres.[47] Additionally, derivatives of glutamic acid, like PBLG, possess a high calcium binding affinity, which could

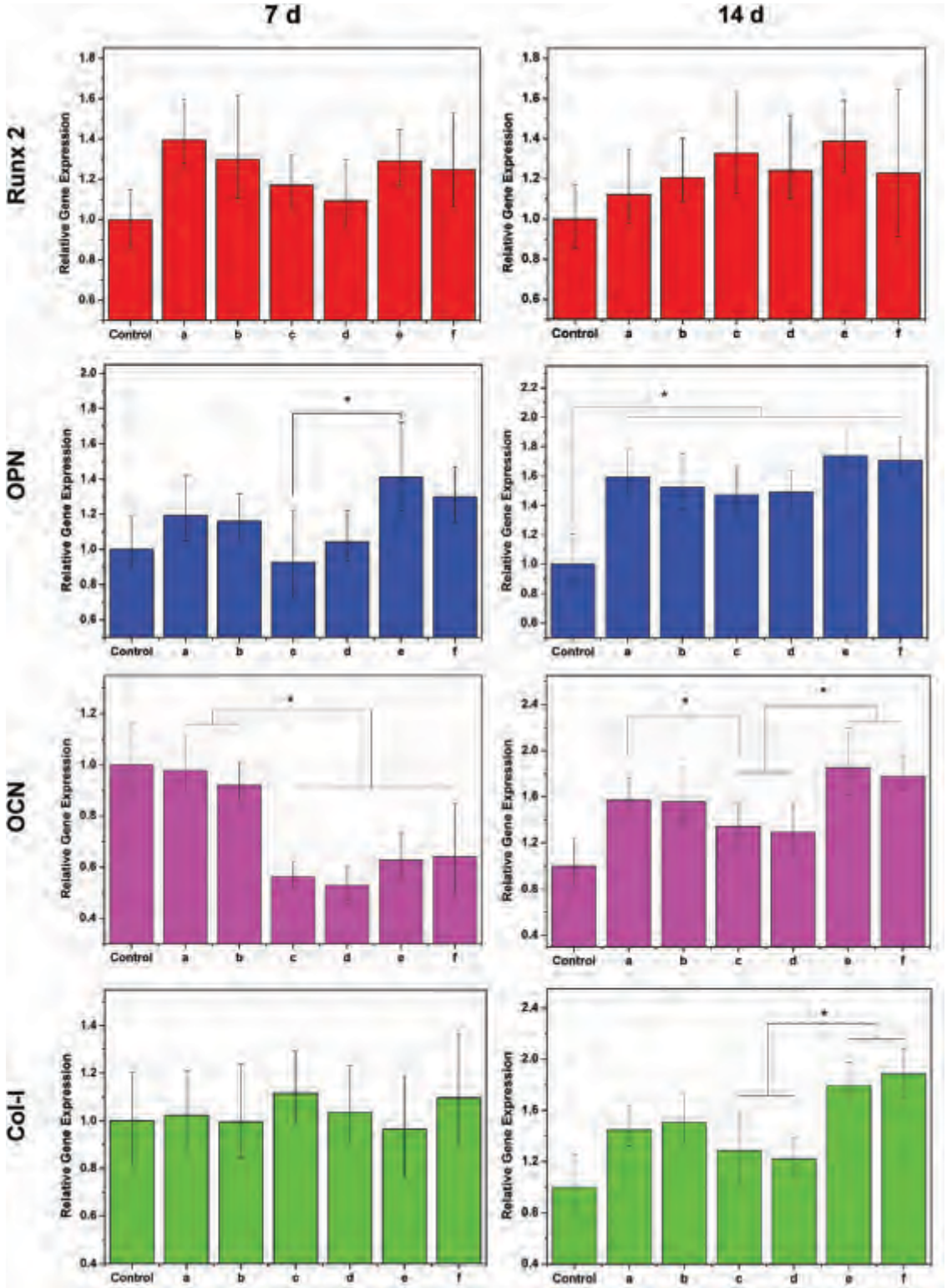

Fig. 9 Real-time qPCR analysis of the osteogenesis-related genes *Runx 2*, *OPN*, *OCN*, and *Col-I* after the cells were cultured for 7 and 14 days on different matrices: (a and b) PBLG-*g*-MHA film with graft amounts of 33% and 50%, (c and d) PLGA/MHA microcarriers with a PLGA component ratio of 33% and 50%, and (e and f) PBLG-*g*-MHA microcarriers with graft amounts of 33% and 50%.

induce osteoblast differentiation and new bone formation.[49] On the other hand, synthesized HA nanoparticles have similarities to the mineral phase of natural bone[50] and promote bone binding and osteoconductivity.[46] Thus, the utilization of HA is necessary for the composite implant designed for bone tissue engineering. Compared to pure PLGA, HA/PLGA exhibited

improved cell proliferation in MC3T3-E1 cell cultures (Fig. 7a). Although the MHA nanoparticles were covered by PBLG by *in-situ* polymerization, the elements Ca and P were still exposed and were detected on the surfaces of microcarriers (Fig. 5c and d). In Fig. S2(a) and (b) (ESI†), on comparison with Fig. 5(a) and (b), the size and surface morphology of the MHA/PLGA microcarriers barely changed. And in Fig. S2(c) and (d) (ESI†), the elements of Ca and P could also be detected. So, the actual difference between the two kinds of microspheres was the organic components of PLGA and PBLG. Thus, we deduced that the combined utilization of PBLG and MHA is beneficial for accelerating the attachment, growth (Fig. 7c and 8) and differentiation (Fig. 9) of pre-osteoblast cells.

Surface roughness is also important for cell attachment.[43] During the fabrication of the PBLG-*g*-MHA microspheres, the organic phase $CHCl_3$ was gradually evaporated and gas pores appeared on the surfaces of the microspheres (as shown in Fig. 5a-3 and b-3). Thus, the surface roughness increased. Porous and rough topographies provide a high surface area for the absorption of cell adhesion proteins from the culture medium and thus help to increase the attachment of cells on the microspheres.[51]

The PBLG-*g*-MHA microcarriers were conveniently fabricated and possessed good biocompatibility and bioactivity. However, the microspheres fabricated by the solvent-evaporation method have relatively low productivity and high size distributions. Accordingly, they do not fully meet the requirements for clinical usage and resulted in poor flow behavior, limiting their utilization in cell rotation culture and tissue engineering. In the future, a static electric field-assisted fabrication method could be utilized to fabricate microcarriers with high productivity and uniformity in particle size distribution.

4. Conclusions

In conclusion, this study demonstrated a promising preparation method for microcarriers as a 3-D cell expansion platform to obtain large quantities of the desired cells and bone regeneration. Biocompatible and biodegradable microspheres composed of the synthetic polypeptide PBLG grafted onto the surface of HA were successfully prepared by a simple and traditional method. *In vitro* pre-osteoblast cell culture revealed better cell proliferation and differentiation on the PBLG-*g*-MHA microcarriers and thus they could be used for cell expansion and might have direct applications as cell-microcarrier injectable complexes. As previously noted, owing to the relatively low productivity and high size distribution of microcarriers in the current research, it is important to explore new fabrication methods to ensure high productivity and particle size uniformity in future studies.

Conflicts of interest

The authors declare no competing financial interest.

Acknowledgements

This research was financially supported by the National Natural Science Foundation of China (Projects 51473164, 51673186 and 51403197), the Program of Scientific Development of Jilin Province (20170520121JH and 20170520141JH), the joint funded program of the Chinese Academy of Sciences and the Japan Society for the Promotion of Science (GJHZ1519), and the Special Fund for Industrialization of Science and Technology Cooperation between Jilin Province and the Chinese Academy of Sciences (2017SYHZ0021).

References

1 M. S. Croughan, J. F. Hamel and D. I. Wang, *Biotechnol. Bioeng.*, 1987, **29**, 130–141.
2 J. M. Melero-Martin, S. Santhalingam and M. Al-Rubeai, *Adv. Biochem. Eng./Biotechnol.*, 2009, **112**, 209–229.
3 K. Song, X. Yan, Y. Zhang, F. Song, M. Lim, M. Fang, F. Shi, L. Wang and T. Liu, *Bioprocess Biosyst. Eng.*, 2015, **38**, 1527–1540.
4 S. M. Badenes, T. G. Fernandes, C. A. Rodrigues, M. M. Diogo and J. M. Cabral, *Methods Mol. Biol.*, 2015, **1283**, 23–29.
5 A. L. van Wezel, *Nature*, 1967, **216**, 64–65.
6 H. P. Tan, D. J. Huang, L. H. Lao and C. Y. Gao, *J. Biomed. Mater. Res., Part B*, 2009, **91B**, 228–238.
7 E. A. Botchwey, S. R. Pollack, E. M. Levine and C. T. Laurencin, *J. Biomed. Mater. Res.*, 2001, **55**, 242–253.
8 J. Malda and C. G. Frondoza, *Trends Biotechnol.*, 2006, **24**, 299–304.
9 R. Chen, S. J. Curran, J. M. Curran and J. A. Hunt, *Biomaterials*, 2006, **27**, 4453–4460.
10 A. Johansson and V. Nielsen, *Dev. Biol. Stand.*, 1980, **46**, 125–129.
11 D. W. Levine, D. I. C. Wang and W. G. Thilly, *Biotechnol. Bioeng.*, 1979, **21**, 821–845.
12 J. Varani, M. Dame, T. F. Beals and J. A. Wass, *Biotechnol. Bioeng.*, 1983, **25**, 1359–1372.
13 Y. Hong, C. Y. Gao, Y. Xie, Y. H. Gong and J. C. Shen, *Biomaterials*, 2005, **26**, 6305–6313.
14 T. L. Gao, N. Zhang, Z. L. Wang, Y. Wang, Y. Liu, Y. Ito and P. B. Zhang, *Macromol. Biosci.*, 2015, **15**, 1070–1080.
15 Y. S. Chen, R. G. Alany, S. A. Young, C. R. Green and I. D. Rupenthal, *Drug Delivery*, 2011, **18**, 493–501.
16 K. B. Lee, K. R. Yoon, S. I. Woo and I. S. Choi, *J. Pharm. Sci.*, 2003, **92**, 933–937.
17 P. Gentile, V. Chiono, I. Carmagnola and P. V. Hatton, *Int. J. Mol. Sci.*, 2014, **15**, 3640–3659.
18 K. D. Newman and M. W. McBurney, *Biomaterials*, 2004, **25**, 5763–5771.
19 M. Savi, L. Bocchi, E. Fiumana, J. P. Karam, C. Frati, F. Bonafe, S. Cavalli, P. G. Morselli, C. Guarnieri, C. M. Caldarera, C. Muscari, C. N. Montero-Menei, D. Stilli, F. Quaini and E. Musso, *J. Biomed. Mater. Res., Part A*, 2015, **103**, 3012–3025.

20 S. S. Kim, M. Sun Park, O. Jeon, C. Yong Choi and B. S. Kim, *Biomaterials*, 2006, **27**, 1399–1409.

21 P. Zhang, Z. Hong, T. Yu, X. Chen and X. Jing, *Biomaterials*, 2009, **30**, 58–70.

22 H. C. Chang, C. Yang, F. Feng, F. H. Lin, C. H. Wang and P. C. Chang, *J. Formosan Med. Assoc.*, 2017, DOI: 10.1016/j.jfma.2017.01.005. Q9

23 M. Wang, *Biomaterials*, 2003, **24**, 2133–2151.

24 I. Manjubala, I. Ponomarev, I. Wilke and K. D. Jandt, *J. Biomed. Mater. Res., Part B*, 2008, **84B**, 7–16.

25 H. Yuan, K. Kurashina, J. D. de Bruijn, Y. Li, K. de Groot and X. Zhang, *Biomaterials*, 1999, **20**, 1799–1806.

26 E. Hinoi, T. Takarada and Y. Yoneda, *J. Pharmacol. Sci.*, 2004, **94**, 215–220.

27 P. Markland, G. L. Amidon and V. C. Yang, *Int. J. Pharm.*, 1999, **178**, 183–192.

28 H. Y. Tian, W. Xiong, J. Z. Wei, Y. Wang, X. S. Chen, X. B. Jing and Q. Y. Zhu, *Biomaterials*, 2007, **28**, 2899–2907.

29 H. Y. Tian, L. Lin, J. Chen, X. S. Chen, T. G. Park and A. Maruyama, *J. Controlled Release*, 2011, **155**, 47–53.

30 R. Ravichandran, J. R. Venugopal, S. Sundarrajan, S. Mukherjee and S. Ramakrishna, *Biomaterials*, 2012, **33**, 846–855.

31 J. C. Wei, A. X. Liu, L. Chen, P. B. Zhang, X. S. Chen and X. B. Jing, *Macromol. Biosci.*, 2009, **9**, 631–638.

32 L. Liao, S. Yang, R. J. Miron, J. Wei, Y. Zhang and M. Zhang, *PLoS One*, 2014, **9**, e105876.

33 N. Zhang, T. L. Gao, Y. Wang, Z. L. Wang, P. B. Zhang and J. G. Liu, *Mater. Sci. Eng., C*, 2015, **46**, 158–165.

34 Y. Yao, W. W. Li, S. B. Wang, D. Y. Yan and X. S. Chen, *Macromol. Rapid Commun.*, 2006, **27**, 2019–2025.

35 X. Y. Qiu, Y. D. Han, X. L. Zhuang, X. S. Chen, Y. S. Li and X. B. Jing, *J. Nanopart. Res.*, 2007, **9**, 901–908.

36 X. Y. Qiu, Z. K. Hong, J. L. Hu, L. Chen, X. S. Chen and X. B. Jing, *Biomacromolecules*, 2005, **6**, 1193–1199.

37 P. Zhang, H. Wu, H. Wu, Z. Lu, C. Deng, Z. Hong, X. Jing and X. Chen, *Biomacromolecules*, 2011, **12**, 2667–2680.

38 J. Feng, M. Chong, J. Chan, Z. Y. Zhang, S. H. Teoh and E. S. Thian, *J. Biomater. Appl.*, 2014, **29**, 93–103.

39 E. Boanini, P. Torricelli, M. Gazzano, R. Giardino and A. Bigi, *Biomaterials*, 2006, **27**, 4428–4433.

40 Z. Wang, L. Chen, Y. Wang, X. Chen and P. Zhang, *ACS Appl. Mater. Interfaces*, 2016, **8**, 26559–26569.

41 G. J. Lai, K. T. Shalumon, S. H. Chen and J. P. Chen, *Carbohydr. Polym.*, 2014, **111**, 288–297.

42 T. L. Gao, W. W. Cui, Z. L. Wang, Y. Wang, Y. Liu, P. S. Malliappan, Y. Ito and P. B. Zhang, *RSC Adv.*, 2016, **6**, 20202–20210.

43 B. Setzer, M. Bachle, M. C. Metzger and R. J. Kohal, *Biomaterials*, 2009, **30**, 979–990.

44 K. Atluri, D. Seabold, L. Hong, S. Elangovan and A. K. Salem, *Mol. Pharmaceutics*, 2015, **12**, 3032–3042.

45 Q. Q. Hoang, F. Sicheri, A. J. Howard and D. S. C. Yang, *Nature*, 2003, **425**, 977–980.

46 N. H. Dormer, Y. Qiu, A. M. Lydick, N. D. Allen, N. Mohan, C. J. Berkland and M. S. Detamore, *Tissue Eng., Part A*, 2012, **18**, 757–767.

47 J. J. Fang, Q. Yong, K. X. Zhang, W. T. Sun, S. F. Yan, L. Cui and J. B. Yin, *J. Mater. Chem. B*, 2015, **3**, 1020–1031.

48 H. Shen, X. X. Hu, F. Yang, J. Z. Bei and S. G. Wang, *Acta Biomater.*, 2010, **6**, 455–465.

49 R. Ravichandran, J. R. Venugopal, S. Sundarrajan, S. Mukherjee and S. Ramakrishna, *Biomaterials*, 2012, **33**, 846–855.

50 Y. D. Liu, H. T. Cui, X. L. Zhuang, P. B. Zhang, Y. Cui, X. H. Wang, Y. Wei and X. S. Chen, *Macromol. Biosci.*, 2013, **13**, 356–365.

51 K. M. Woo, V. J. Chen and P. X. Ma, *J. Biomed. Mater. Res., Part A*, 2003, **67A**, 531–537.